21 *Egypt. J. Chem*. **55**, No. 3, pp. 307-319 (2012)

Characterization and Catalytic Activity of Ni, Mo and Ni-Mo Supported on Al_2O_3 Systems

E.M. Ezzo, M.A. El-Kherbawi*, M.K. El-Aiashy and R.M. Mansour
Chemistry Department, Faculty of Girls, Ain Shams University,
Heliopolis, Cairo, Egypt.

A SERIES of Ni, Mo and Ni-Mo supported alumina catalysts were prepared for investigating the interaction between Ni and Mo in terms of their structural properties and catalytic activities.The samples were prepared by wet impregnation with 20 wt% total loading (NiO+MoO) in different molar ratios. The investigated samples were characterized by DSC, TGA, XRD and BET. The catalytic activity and selectivity were studied using isopropanol conversion in flow system under normal pressure at temperature range300-360°C and space velocity 11.60-18.40 ml.min^{-1}. The reaction products were analyzed using gas liquid chromatography. The main product is acetone and the activation energy is calculated over the investigated catalysts. The results demonstrate that Mo loading enhances formation of $NiAl_2O_4$ phase.

Keywords: Isopropanol, Dehydration, $NiAl_2O_4$, Bimetal oxide and BET.

In the last decade, a great interest has been observed in the development of highly selective catalysts for the transformation of light alkanes into more valuable organic compounds(1). One of the most important options for enhancing the activity and/or products selectivity for isopropanol conversion is the use of bimetallic systems including bimetals or bimetal oxides(2-6). Literatures have dealt with the composition change of catalysts consisting of alumina supported nickel(7-9). They observed that, nickel oxide present on the catalyst surface reacts with the support to create the $NiAl_2O_4$ spinel which contributes to increase the catalyst mechanical resistance and the catalyst activity at higher temperature. Extensive literatures were describing the Ni-Mo/Al_2O_3 systems in steam reforming of hydrocarbons and hydrodesulphurization(10-12). It was found that there is a synergetic interaction between active Ni-sites and MoO_x species leading to change in metal surface area and activities compared to monometallic Ni/Al_2O_3. At other extreme, at higher total metal loadings and low Ni:Mo ratios, partial coverage of Ni sites by MoO_x species occurs resulting in loss of total activity. At intermediate metal loadings and Ni:Mo ratios, electron transfer from MoO_x species active Ni sites dominates leading to increases in specific activity with increasing Mo content.

Isopropanol decomposition has long been considered as chemical prop reaction for catalytic activity. It has been reported that IPA undergoes

---

*Corresponding author: E-mail address: magdaelkherbawi@hotmail.com dehydrogenation to acetone over basic sites or dehydration to propylene over acidic sites (13-22). Moreover availability of surface redox sites ($M^{n+}/M^{(n-1)+}$) can also enhance IPA dehydrogenation(19). Thus, the dehydrogenation of IPA is not solely dependent on the availability of surface basic sites. Similar to methanol and ethanol, isopropanol undergoes also bimolecular reaction caused by the coupling of two surface isopropoxide species to give isopropyl ether on acidic surface sites(23), or bimolecular dehydrogenation on basic sites to give diethyl ether(24-28).

The objective of this paper is to characterize the structures and textural characteristics of Ni/Al_2O_3, Mo/Al_2O_3 and co-impregnated $Mo\text{-}Ni/Al_2O_3$ oxide catalysts to investigate the metal support and metal-metal support interaction by measuring surface properties, DSC, XRD and BET. The activity and selectivity were studied using isopropanol conversion (IPA) as model reaction in flow system under normal pressure. The kinetic parameters were calculated.

Experimental

Catalyst preparation

Aluminum nitrate solution was used to prepare alumina gel which dried at 120˚C and calcined for 4hr at 500˚C (28,29). Known weight of alumina was impregnated by definite amount nickel nitrate and ammonium heptamolybedate solution with the constant total loading 20%, to produce Ni/AlO I, Ni-Mo/AlO (II-V) and Mo/AlO VI.The solids were crushed and calcined at 500, 600 and700˚C . The designation of the prepared solids and their thermal products were described in Table 1.

TABLE 1. Catalysts composition and textural properties .

Catalysts	Catal. compoition (wt. %)			Calcin. temp.,°C	Surface area (m^2g^{-1})	Pore volume ($cm^3.g^{-1}$)	Mean pore radius(A˚)	C_{BET}, const.	Cryst.	Size L (nm)	
	NiO	Mo	Al_2O_3						$NiAl_2O_4$	NiO	MoO_3
Ni/AlOI 1	20	–	80	500	89.54	0.15	14.10	188.30	34.9	29.4	----
Ni/AlOI 2				600	120.65	0.18	31.68	31.00	50.5		
Ni/AlOI 3				700	73.53	0.12	14.10	188.40			
Ni-Mo/AlOII 1	18	2	80	500	121.73	0.21	62.24	141.40	18	24.9	---
Ni-Mo/AlOII 2				600	117.94	0.19	49.68	31.90	12.2		
Ni-Mo/AlOII 3				700	88.02	0.16	71.24	125.00	23.7		
Ni-Mo/AlOIII 1	14	6	80	500	131.07	0.20	71.24	191.00	29.9	29.8	---
Ni-Mo/AlOIII 2				600	138.89	0.18	140.98	500.30	47.7		
Ni-Mo/AlOIII 3				700	96.22	0.18	71.24	238.80			
Ni-Mo/AlOIV 1	8	12	80	500	85.49	0.11	14.10	591.80	45.5	55.8	---
Ni-Mo/AlOIV 2				600	157.28	0.21	31.68	22.60	20.7		
Ni-Mo/AlOIV 3				700	72.98	0.12	71.24	299.60	22.3		
Ni-Mo/AlOV 1	4	16	80	500	118.23	0.17	14.10	180.40	----	11.9	----
Ni-Mo/AlOV 2				600	226.57	0.29	36.26	12.20		24.0	
Ni-Mo/AlOV 3				700	82.76	0.13	14.10	340.20		24.0	
Mo/AlOVI 1	–	20	80	500	104.15	0.13	14.10	148.70	----	----	4.5
Mo/AlOVI 2				600	227.66	0.31	36.26	16.00			26.5
Mo/AlOVI 3				700	85.83	0.14	14.10	294.80			20.4

Characterization

Thermogravimetic analysis TGA and differential scanning calorimetry (DSC) were measured for fresh portions of all solid samples in the temperature range 0 up to 1000˚C using thermo balance. The data were obtained using SETARAM Labsys^{TM} TG-DSC 16.The rate of heating of the samples 5˚C / min and flow rate of argon was 30 ml/min.

The surface properties, for all samples calcined at 500, 600 and 700˚C were estimated by using Quanta chrome Nova 1000, Win 2 by adsorption of nitrogen at -196˚C on the investigated samples previously degassed at 250˚Cunder high vacuum atmosphere for 2 hr.

X-ray diffraction patterns for the calcined samples were recorded at room temperature by BRUKER D8 diffractometer, with CuKα radiation of a wave length of 1.5405 A˚ at 40 kV, 40 mA. 2θ from 4 to 70˚ and scan rate of 2˚/min.

Catalytic conversion of isopropanol

The catalytic activity was carried out over the samples calcined at 500˚C, using isopropanol conversion as a prop reaction at temperature range 280 -360˚C in flow system(28,29) under normal condition. The reactant (pure isopropanol) was introduced using a microdose pump (Unipan 335A) with space velocity 11.60-18.7x10^{-2} ml/ min. Catalyst sample (1ml) was introduced into a quartz reactor between two silica wool beds and activated in situ by calcination at 500˚C for 4 hr in a current of dry air free from CO_2, then cooled down to the experimental temperature. The gaseous and liquid products of the catalytic reaction were analyzed using programmed gas- liquid chromatography (Perkin Elmer 8600), double flame ionization detector on a column 5% CW1540 on CSORB (Gaw-DMCs) which was applied for alcohols using pure nitrogen as a carrier gas.

Results and Discussion

Thermal behavior

The TGA curves (not illustrated) for all investigated samples show two main steps corresponding to removal of water of hydration of nickel nitrate hexahydrate, ammonium heptamolybedate tetrahydrate and volatilization of ammonia. The second step represents the complete decomposition of nickel nitrate into nickel oxide and ammonium heptamolybedate to MoO_3. For the sample Ni-Mo/AlO V an additional peak was observed at 405 ^{o}C which may be attributed to the presence of another form of molybdenum oxide (IV).

The DSC curves of parent samples are given in Fig. 1. Two sets of endothermic peaks were observed for all investigated catalysts located at 97-131 and 374-435˚C. The two peaks are sharp and strong. The first set corresponds to desorption of the physisorbed water and water of crystallization of different precursors. The second strong endothermic peak indicates a complete thermal decomposition of nickel nitrate and ammonium heptamolybedate into NiO and

MoO_3, respectively, with simultaneous liberation of nitrogen oxides and ammonia and then remains constant up to 1000˚C(30). Moreover, sample Ni-Mo/AlOV exhibits an additional peak at 442˚C, this peak is sharp and strong and might be attributed to the presence of MoO_2 as new phase. The endothermic peak relative to thermal decomposition of ammonium heptamolybedate was shifted from 435 to 390˚C for bimetallic samples. These results showed that nickel nitrate enhanced the thermal decomposition of ammonium heptamolybedate into MoO_3. These findings will be confirmed later by XRD.

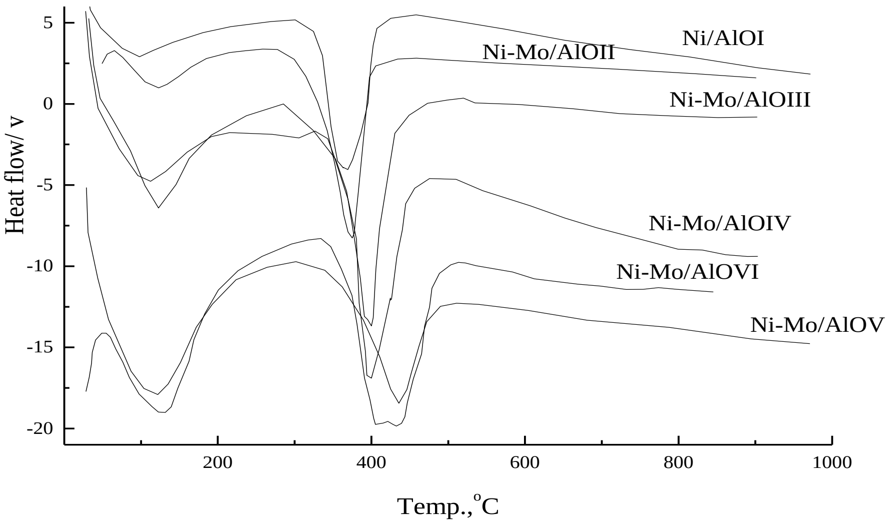

Fig.1. DSC curves of Ni/AlOI, Ni-Mo/AlO(II-V) and Mo/AlOVI catalysts.

Surface characteristics

The specific surface area (S_{BET}), total pore volume and mean pore radius of Ni-Mo/AlO (I-VI) catalysts calcined at 500, 600 and 700˚C were determined from nitrogen adsorption isotherms carried out at -196˚C. The adsorption-desorption isotherms for nitrogen on various solids are illustrated in Fig. 2. All isotherms belong to type II of Brunauer's classification(31-33).The specific surface area S_{BET} was obtained by applying the BET equation. The calculated values determined from linear BET – plots and the mean pore radius are shown in Table 1, which indicates that (i) The S_{BET} of the samples at 500˚C was found to increase by Mo loading until reaching to its maximum value for Ni-Mo/AlOIII then decrease for Ni-Mo/AlOIV1. (ii) The increase in calcination temperature of solids from 500 to 600˚C resulted in a significant increase in their specific surface areas reaching to its maximum value for Ni-Mo/AlOVI2. The observed increase in the specific surface area of catalysts at 600˚C may be attributed to the creation of new pores resulting from complete formation of NiO, MoO_2 and MoO_3(11). (iii) The decrease in the S_{BET} values of solids at 700˚C could be attributed to the sintering process. The sintering process might take place according to the collapse of the pore structure and / or grain growth process together with possible phase transformation(32-35). (iv)The upward deviation of V-t plot indicates the existing of wide pores (mesopores)(33-35) confirmed by the shape of isotherms.

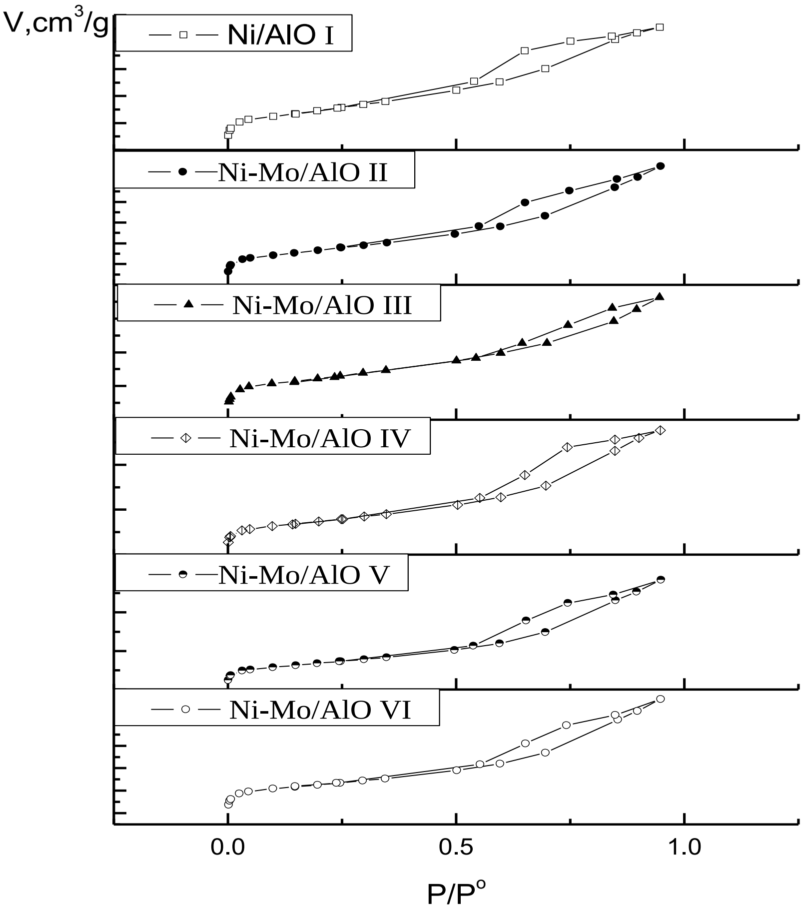

Fig. 2. Adsorption-desorption isotherms of Ni-Mo/AlO systemes .

XRD analysis

XRD patterns of the investigated samples are shown in Fig. 3. They revealed that: (i) Sample Ni/AlOI1 calcined at 500˚C consists of γ-Al_2O_3, NiO and $(NiO_{0.194}Al_{0.806})$ $(Al_{1.194}NiO_{0.806})$ O_4 recorded at 2θ = 62.30, 42.92 and 36.97 (100% intensity), respectively. Further increases of temperature to 600 and 700˚C produce the same patterns. (ii) Catalysts Ni-Mo/AlO (II-IV) 1, show signals recorded at 2θ corresponding to γ-Al_2O_3, NiO and $NiAl_2O_4$ spinel. The formation of $NiAl_2O_4$ spinel may be referred to the increase in Mo loading which acts as catalyst for formation of $NiAl_2O_4$ spinel confirming solid - solid interaction$^{(36-38)}$.

$$Al_2O_3 + NiO \rightarrow NiAl_2O_4$$

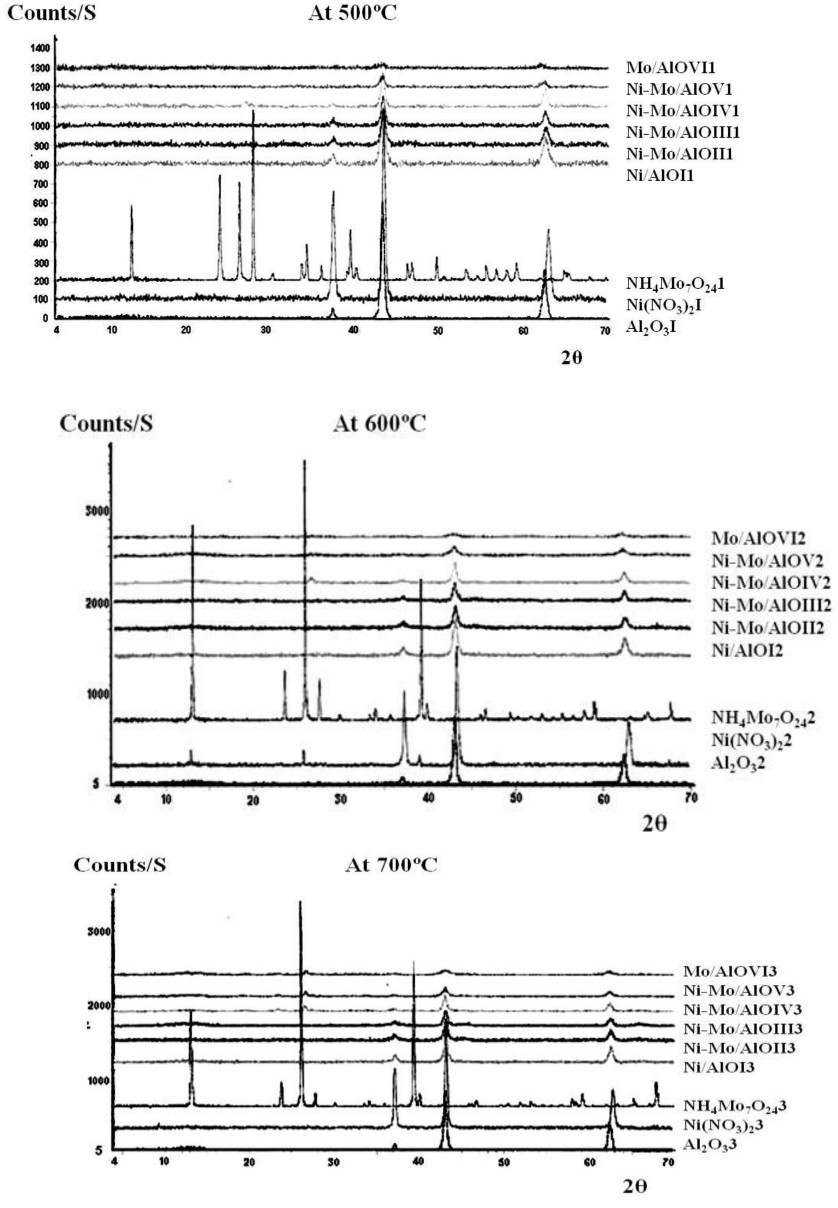

Fig.3.X-ray diffractograms of pure and supported Ni/AlOI, Ni-Mo/AlO(II-V) and Mo/AlOVI solids calcined at 500, 600 and 700 °C.

By increasing calcination temperature, the intensity of $NiAl_2O_4$ decreased and no different behaviors were observed for Ni-Mo/AlO (II, III) 2, 3. (iii) Samples Ni-Mo/AlO IV 2, 3 show the appearance of a new diffraction line at $2\theta = 26.33$ and 23.19 which corresponds to MoO_2 tetragonal lattice structure and MoO_3 monoclinic lattice structure, respectively. (iv) Ni-Mo/AlO V 1, 2 samples calcinated at 500 and 600˚C show only signal of NiO. The absence of any diffraction line of Mo indicates that MoO_3 is actually dispersed as an amorphous phase on the support surface or on the surface of NiO crystallites(16). Further increase in calcinations temperature of Ni-Mo/AlO V 3 to 700˚C stimulated an interaction between Ni and Al_2O_3 yielding $NiAl_2O_4$. So, a portion of Mo added to the investigated system dissolved in the matrices of reacting NiO and Al_2O_3 producing $NiAl_2O_4$(4,38) and the other portion produced MoO_2 and MoO_3 at $2\theta = 26.4$ and 23.17, respectively. (v) For Mo/AlO VI 1, 2 calcined at 500 and 600˚C, show peaks for γAl_2O_3 at $2\theta = 62.02$ and 62.17, respectively. Further increasing in calcinations temperature, a new peak appears at $2\theta = 24.19$ which indicates the formation of $Al_2(MoO_4)_3$ spinel as a result of solid-solid interaction (5).

Table 1 illustrates the increase of crystal size (d) of $NiAl_2O_4$ phase by increasing the Mo loading at 500˚C while the surface area for Ni-Mo/AlO IV catalyst decrease by 30 % than the Ni-Mo/AlO II catalyst. $NiAl_2O_4$ phase formed did not modify its surface characteristics but may result in an increase in the degree of dispersion of MoO_3 crystallites via decreasing their particle size.

Catalytic activity measurements

The catalytic conversion of IPA was carried out over the calcined catalysts at 500˚C. The experimental temperatures were chosen to be in the range 280 - 360˚C using a flow system under normal pressure. The rate of IPA decomposition at each experimental temperature was studied at space velocity 11.60-18.40 $x10^{-2}$ ml/min, the obtained results indicated that the rate of conversion is independent of the time of contact (τ, min) at all selected temperatures (the figure not illustrated). The analysis of reaction products emphasized the presence of acetone, propene, acetaldehyde, diethyl ether and diisopropylether; the latter produced only at high temperature. But acetone is the main product over all samples(38). These indicate that IPA conversion proceeds through two main routes; i) mainly dehydrogenation to produce acetone, acetaldehyde and diethyl ether and/or ii) dehydration to produce propene or diisopropyl ether.

The apparent activation energy was calculated according to Arrhenius equation for each catalyst at constant space velocity of IPA. Apparent activation energy for IPA dehydration and dehydrogenation is 80 ±4 kJ.

Figure 4 reveals the selectivity % for acetone and propene formation over the investigated catalysts at the selected temperatures. It is observed that; (i) Acetone is the selective product over all investigated samples. (ii) Ni-Mo/AlO II and Ni/AlO I catalysts are the most selective catalysts for acetone formation where the selectivity % of Ni-Mo/AlO II not greatly affected by temperature may be due to the presence of NiO species. (iii) Ni-Mo/AlO V catalyst is the most selective one for propene at 280, 340°C where Mo/AlO VI catalyst is the most selective at 300, 340 and 360 °C due to the presence of MoO_3 species which has acidic character. (v) For bimetallic catalysts Ni-Mo/AlO (II-V), increasing of Mo loading resulted in a progressive increase in propene selectivity % reaching to its maximum value for Ni-Mo/AlO V catalyst which may be attributed to the formation of $NiAl_2O_4$ phase(37,38). So, the observed increase in the dehydration % may be attributed to the increase in the degree of dispersion of MoO_3 phase(4,5). However, as indicated from XRD measurements that the Ni-Mo/AlO V catalyst calcined at 500˚C contains NiO. So, the observed decrease in dehydration % for Ni-Mo/AlO V catalyst may be attributed to absence of $NiAl_2O_4$ phase. It can be concluded that the conversion of IPA over the investigated systems Ni-Mo/AlO (II-IV) catalysts is mainly dependent on the formation of $NiAl_2O_4$ phase, MoO_2 and MoO_3 rather than the surface characteristics of the system investigated.

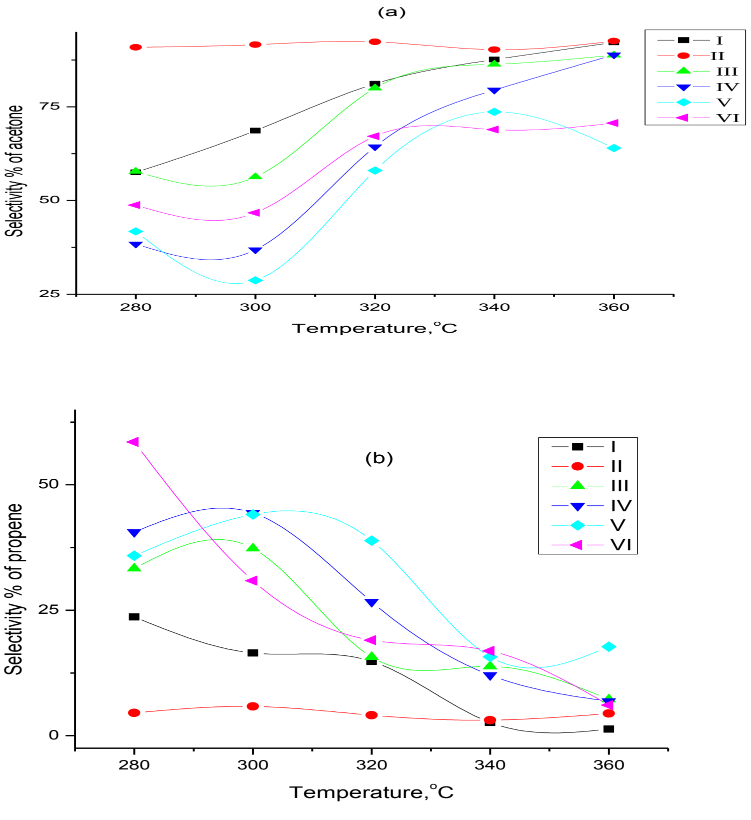

Fig. 4. Variation of selectivity % of acetone (a) and propene (b) with experimental temperature over Ni/AlOI, Ni-Mo/AlO (II-V) and Mo/AlOVI catalysts calcined at 500°C.

Figure 5. shows the variation of specific activity of isopropanol conversion over used catalysts with temperatures, it is obvious that the specific activity increased by temperature and Ni-Mo/AlO IV, Ni/AlO I catalysts show the highest specific activity at all experimental temperatures.

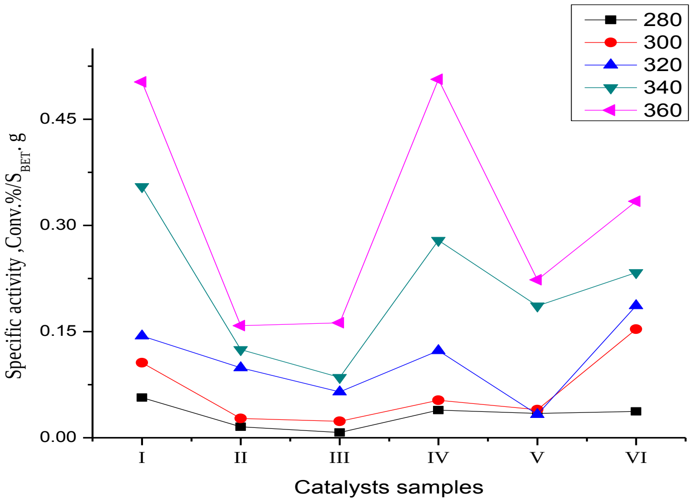

Fig. 5. Effect of temperatures on the specific activity of isopropanol conversion over Ni/AlOI, Ni-Mo/AlO (II-V) and Mo/AlOVI catalysts calcined at 500°C.

Conclusions

1.Solid interaction occurred between NiO and γ-Al_2O_3 at 500 °C to form $NiAl_2O_4$ which increased by Mo loading.The surface area the pore size of the investigated samples give higher values at 600 °C and the pores have mesopores in nature. The different loading ratio of Ni: Mo affected the intensities of mesopores peaks.

2.XRD for mono-oxide systems Ni/AlO I indicate the formation of γ-Al_2O_3, NiO and $NiAl_2O_4$ and for MoO /AlO VI, MoO_3, MoO_2 and $MoAl_2O_4$ (at700 °C). Characterization for bimetal oxide Ni-Mo/Al_2O_3 (II-V) emphasized the formation of γ-Al_2O_3, NiO and $NiAl_2O_4$ while MoO_3or $MoAl_2O_4$ were not detected at lower concentration of Mo. As Mo loading increases MoO_3 can be detected. Moreover, new phase of MoO_2 appears for catalyst Ni-Mo/Al_2O_3V which can be attributed to the existence of Ni species.

3.BET data emphasized that the surface area and pore size distribution were affected by Ni:Mo wt ratios % and calcinations temperature. The enhancement of surface area by Mo loading can be explained by textural promotion of Ni particle distribution by MoO_x species which act as diluents of the catalyst matrix.

4. Ni/AlOI, Ni-Mo/AlOIV catalysts are the most active and exhibit the highest selectivity for acetone formation which may be attributed to presence of NiO species while Mo/AlOVI catalyst was most active for dehydration reaction which may be attributed to the presence of MoO_3 species. The changes of selectivity of Ni-Mo catalysts are of significant importance where the addition of Mo resulted in a progressive increase of selectivity to dehydration and formation of $NiAl_2O_4$. The specific activity and selectivity of the investigated catalyst depends on nature of the catalyst, its composition, experimental temperature and textural properties

References

1. **Abello, M.C., Gomez, M.F., Ferretti, O.,** Mo\γ-Al_2O_3 catalysts for oxidative dehydrogenation of propane: Effect of Mo loading. *Appl.Catal. A: General* **207**, 421 (2001).

2. **Guczi, L.,** Structure and promotion of bimetallic catalysts: Activity and selectivity. *Catal. Lett*. **7,** 205 (1990).

3. **Adesina, A.A.** Hydrocarbon synthesis via Fischer-Tropsch reaction: travails and triumphs. *Appl. Catal. A: General,* **138**, 345 (1996).

4. **Aksoylu, A.E., Isli, A.I., and Önsan, Z.I.,** Interaction between nickel and molybdenum in Ni–Mo/Al_2O_3 catalysts: III.: Effect of impregnation strategy. *Appl. Catal. A: General,* **183,** 357 (1999).

5. **Borowiecki, T., Giecko G. and Pancyzyk, M.,** Effects of small MoO_3 additions on the properties of nickel catalysts for the steam reforming of hydrocarbons II. Ni-Mo/Al_2O_3 catalysts in reforming, hydrogenolysis and cracking of n-butane**.** *Appl. Catal. A: General,* **230,** 85 (2002).

6. **Yoshida, N., Yamamoto, T., Minoguchi, F. and Kishimoto, S.,** Effect of hydrogen on carbon deposition from carbon monoxide on nickel catalyst. *Catal. Lett*. **23,** 237 (1994).

7. **Zielinski, J.,** Morphology of coprecipitated nickel/alumina catalysts with low alumina content. *Appl.Catal*. **A**. **94**, 107(1993).

8. **Lamber, R. and Schulz-Ekloff, G.,** On the microstructure of the coprecipitated Ni-Al_2O_3 catalysts. *J.Catal*. **146**, 601 (2006).

9. **Oukacine, L., Gitzhofer, F., Abatzoglou, N. and Gravelle, D.,** Application of the induction plasma to the synthesis of two dimensional steam methane reforming Ni/Al_2O_3 catalyst. *Surface & Coating Technol*. **201**, 2046 (2006) .

10. **Andonova, S., Vladov, Ch., Kunev, B., Mitov, I., Tyuliev, G., Fierro, J. L.G., Damyanova, S. and Petrov, L.,** Study of the effect of mechanical- chemical activation of Co-Mo\γ-Al_2O_3 and Ni-Mo\γ-Al_2O_3 catalysts for hydrodesulfurization. *Appl.Catal.A:G*. **298**, 94 (2006).

11. **Chen, Y.G., and Ren, J.,** Conversion of methane and carbon dioxide into synthesis gas over alumina-supported nickel catalysts. Effect of Ni-Al_2O_3 interactions. *Catal. Lett*. **29,** 39 (1994).

12. **Diez, V.K., Apesteguia, C.R. and Dicosimo, J.I.,** Acid–base properties and active site requirements for elimination reactions on alkali-promoted MgO catalysts. *Catal. Today*, **63**, 53 (2000).

13. **Hathaway, P.E. and Davis, M.E.,** Base catalysis by alkali-modified zeolites : II. Nature of the active site. *J.Catal*. **116,** 279 (1989).

14. **Gervasini, A. and Auroux A.,** Acidity and basicity of metal oxide surfaces II. Determination by catalytic decomposition of isopropanol. *J. Catal*. **131,**190 (1991).

15. **Mckenzie, A.L., Fishel, C.T. and Davis, R.J.,** Investigation of the surface structure and basic properties of calcined hydrotalcites. *J. Catal*. **138,** 547 (1992).

16. **Gervasini, A., Fenyvesi, J. and Auroux, A.,** Study of the acidic character of modified metal oxide surfaces using the test of isopropanol decomposition. *Catal.Lett*. **43,** 219 (1997).

17. **Aramendia, M.A., Borau, V., Jimenez, C., Marinase, J.M., Porras, A. and Urbano, F.J.,** Magnesium oxides as basic catalysts for organic processes: Study of the dehydrogenation–dehydration of 2-propanol. *J.Catal*. **161**, 829 (1996).

18. **Bej, S.K., Bennet, C.A. and Thompson, L.T.,** Acid and base characteristics of molybdenum carbide catalysts. *J. Appl.Catal. A: G*. **250**, 197 (2003).

19. **Martin, D. and Duprez, D.,** Evaluation of the acid-base surface properties of several oxides and supported metal catalysts by means of model reactions. *J. Mol. Catal. A: Chem*. **118**,113 (1997).

20. **Kulkarni, D. and Wachs I.E.,** Isopropanol oxidation by pure metal oxide catalysts: number of active surface sites and turnover frequencies. *J. Appl. Catal*. **A: G 237**, 121 (2002).

21. **Ai, M. and Suzuki, S.,** Oxidation activity and acidity of MoO_3---P_2O_5 catalysts. *J.Catal*. **30**, 362 (1973).

22. **Rekoske, J.E. and Barteau, M.A.,** Kinetics and selectivity of 2-propanol conversion on oxidized anatase TiO_2. *J. Catal*. **165,** 57 (1997).

23. **Hassan, M.A., Zaki, M.I. and Pasupulety, L.,** A spectroscopic investigation of isopropanol and methylbutynol as infrared reactive probes for base sites on polycrystalline metal oxide surfaces. *J. Molec. Catal. A: Chemical* **178**, 125 (2002).

24. **Velu, S. and Gangwal, S.K.,** Synthesis of alumina supported nickel nanoparticle catalysts and evaluation of nickel metal dispersions by temperature programmed desorption. *Solid State Ionics*, **177**, 803 (2006).

25. **Geoffrey, C.B., Halawy, S.A., Abd Elsalam, M.Kh., Hassan, E.A. and Ragih, H.M.,** MoO_3—Fe_2O_3 catalysts: Characterization and activity for isopropyl alcohol decomposition. *J. Chem.Technol.Biotechnd*. **59**, 181(1994).

26. **Pengpanich, S. Meeyoo, V. and Rirksomboon, T.,** Methane partial oxidation over Ni/CeO_2–ZrO_2 mixed oxide solid solution catalysts. *Catal. Today,* **93-95**, 95(2004).

27. **DiCosimo, J.I., Diez, V.K. and Apesteguia, C.R.,** Base catalysis for the synthesis of α,β-unsaturated ketones from the vapor-phase aldol condensation of acetone. *Appl.Catal.* ***A:G*** **137**,149 (1996).

28. **Ezzo, E., El-kherbawi, M.A. and El-Aiashy, M.K.,** Surface and catalytic activities on Pt\Al and Pd\Al catalysts for cumene conversion. *Mans.Sci.Bull. (A Chem.)* **31,**13.11 (2004).

29. **Ezzo, E.M., Mazhar, H.S., Ali, S.A. and El-Aiashy M.K.,** Study on the dependence of the activity of the conversion of hydrocarbons on the metal content of the catalyst. *J. Materials Letters,* **28**, N323 (1996).

30. **Souza, G.L., Santos, A.C., Lorate, D.A. and Farojr, A.C.,** Characterization of Ni-Mo/Al_2O_3 catalysts prepared by simltaneous impregnation of the active components. *Catal.Today,* **5**, 451(1989).

31. **Brunauer, S., Deming, W.S. and Deming, E.T.,** On a theory of the van der waals adsorption of Gases. *J.Am.Chem.Soc*. **62**, 1723(1940).

32. **Sing, K.S.W.,** IUPAC reporting physisorption data for gas/solid system. *pure Appl.Chem*. **57,** 603 (1985).

33. **Gregg, S.J. and Sing, K.S.W.,** *Adsorption, Surface Area and Porosity.*" Academic Press Inc., London (1982).

34. **Borowiecki, T., Gac, W. and Denis, A.,** Effects of small MoO_3 additions on the properties of nickel catalysts for the steam reforming of hydrocarbons: III. Reduction of Ni-Mo/Al_2O_3 catalysts. *Appl.Catal. A: G*. **270**, 27(2004).

35. **Pantaleo, G., Liotta, L.F., Venezia, A.M., Deganello, G., Ezzo, E.M., El Kherbawi, M.A. and Atia, H.,** Support effect on the structure and CO oxidation activity of Cu-Cr mixed oxides over Al_2O_3 and SiO_2. *Mater. Chem. and Phys*. **114**, 604 (2009).

36. **Deraz, N.M., Selim, M.M. and Ramdan, M.** Processing and properties of nanocrystalline Ni and NiO catalysts. *Mater. Chem.and Phys*. **113**, 269 (2009).

37. **Deraz, N.M., El-Aiashy, M.K. and Ali, Suzan A.,** Noval preparation and physicochemical characterization of a nanocrystalline cobalt ferrite system. *Adsorp.Scien. & Techn*. **27,** 797(2009).

38. **Elkherbawi, M.A.,** Physical and catalytic properties of solids produced from solid-solid interactions between NiO and Fe_2O_3 system doped with Ag_2O. *J. Amer. Scien.***6** (10), 470 (2010).

Received 5/ 8 /2012;
accepted 2/12/2012)

دراسة النشاط الحفزى والتركيبى للنيكل والموليبدنم والنيكل- موليبدنم المحمل على الالومينا

عصام محمد عزو ، ماجدة عبد الباسط الخرباوى ، مها كامل العياشى ورحاب منصور
قسم الكيمياء – كلية البنات – جامعة عين شمس – القاهرة – مصر.

تم تحضير سلسلة من حفازات NiO/Al_2O_3 و MoO_3/Al_2O_3 و $NiO-MO_3/Al_2O_3$ بنسبة كلية 20٪ بالوزن بطريقة التشبع لدراسة اثر وجود الموليبدنم على النيكل ودراسة الخواص الحرارية للعينات المحضرة بواسطة التحلل الحرارى والوزنى التفاضلى بالاضافة الى دراسة الصفات التركيبية بواسطة حيود طيف الاشعة السينية والقياسات السطوحية باستخدام BET.

تمت دراسة النشاط الحفزى والانتقائى للعينات المحضرة بدراسة تحولات الايزوبروبانول فى جهاز التدفق المستمر عند الضغط الجوى ودرجة حرارة 300-360^o مئوية وتيار متدفق من الايزوبروبانول من $18.4-11.6 \times 10^{-2}$ مللى ليتر/دقيقة وبتحليل نواتج التفاعل باستخدام جهاز الفصل الكروماتوجرافى اوضحت نتائج التفاعل ان الناتج الرئيسى هو الاسيتون وتم حساب طاقة التنشيط للتفاعل. واكدت النتائج ان تحميل الموليبدنم يزيد من تكوين مركب $NiAl_2O_3$.